Bridging molecular-scale interfacial science with continuum-scale models

Abstract

Introduction

Fig. 1: Schematic representation of surface complexation modeling.

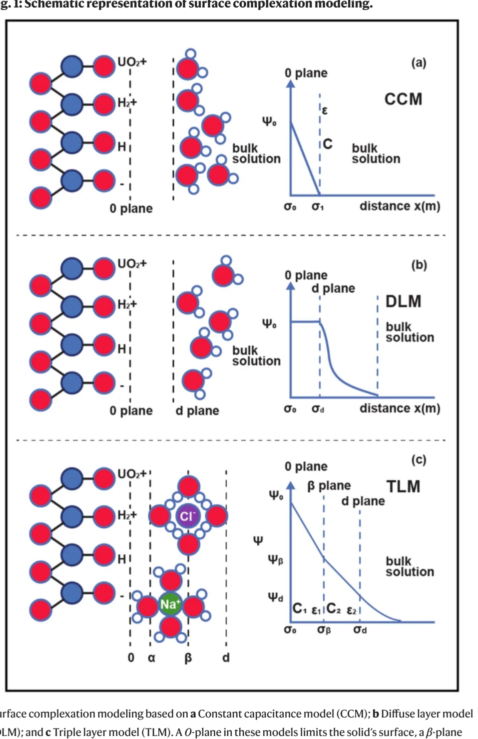

Fig. 2: Calculated Gouy-Chapman Stern potential.

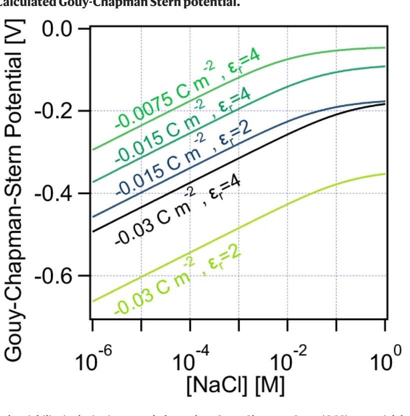

Furthermore, conventional SCMs describe surface properties and reactivities with a single surface acidity constant and surface complexation constant for a given surface and adsorbate (the more advanced SCMs may go as far as to incorporate two- or three-site models with distinct acidity and/or complexation constants). However, new experiments consistently show that nominally similar surface sites (e.g., Si-OH, see ref. [7]) have vastly different reactivities, which are defined by multiple factors: surface structure, hydrogen bonding in adjacent solution, the surface neighbor species, and aqueous composition. Because continuum-scale simulations rely on empirically fit coefficients to approximate parameter values, they often do not capture experimentally measured outcomes. As we will show below, the mismatch in predicted *vs.* experimentally determined parameters can span orders of magnitude.

The other types of continuum-scale reactive models, which are often utilized in important applications such as nuclear waste storage, are reactive transport models (RTMs) that couple transport equations with chemical reactions, including equilibrium constants and kinetic rate laws. Similar to SCMs, equilibrium constants used in RTMs do not fully reflect the reality of a solid–water interface, where isolated surface sites can have dramatically different reactivities. Furthermore, to model the dissolution of solid phases in RTMs average rates or rate constants are selected[8,9], whereas experimental evidence indicates that the effective dissolution rate consists of contributions from specific surface sites, where the rates are vastly different[10]. Because surface structure is dynamic, rates may also vary with time[11], with reaction Gibbs free energy[12], and with flow rate[13]. Accordingly, reaction rates may vary several-fold for the same crystalline solid, depending on the molecular, crystallographic, and topographic details of their surfaces that change dynamically in time. Therefore, reaction rates are best described by distributions of possible/probable values and not by a singular discrete number.

This Perspective argues that, in place of ensemble averaged constants as input parameters, *probability distributions* are needed to formalize chemical phenomena at interfaces to reflect their heterogeneous nature in SCMs, RTMs, and other continuum-scale models. Current state-of-the-art modeling approaches apply homogeneous chemistry concepts to heterogeneous systems, limiting their applicability and predictive power. A probabilistic approach that captures the stochastic nature of surface sites offers a path forward to bridge detailed molecular-scale information with the continuum-scale models of complex systems. We will show that using probability distributions is appropriate for representing the "surface landscape", (i.e., the stoichiometry of surface sites, surface charge distributions, and surface topologies), as well as equilibrium constant values and reaction rates. This approach provides a new paradigm that we hypothesize will create a more robust predictive power in continuum-scale models by capturing the wealth of molecular-scale information that is available for interfacial systems. Using molecular-scale information in continuum-scale simulations will advance our capability to model environmental fate and transport, soil system evolution, and to elevate the design and optimization of electrochemical and catalytic processes, desalination membranes, and carbon- and ion-selective capture materials. Achieving this probabilistic approach requires not just advancements in the capabilities of SCMs and RTMs, but also the continued efforts of experimentalists and computational chemists to elucidate molecular details and reactivities of solid–water interfaces.

Molecular details matter

In this section we will illustrate that a surface is not one reactant but instead a combination of different reactants that are distinct, interdependent, and changing. Recent scientific advances have led to molecular descriptions of interfaces of specific solid–water systems that challenge traditional mean-field models of charged surfaces (see Bañuelos et al. for a comprehensive review)[7]. These studies highlight that molecular details matter as surfaces are heterogeneous at the molecular-scale and cannot be conceptualized as a single "reactant" in interfacial chemistry descriptions. The selected advances illustrated here have been facilitated by new capabilities in scanning probe, synchrotron-based X-ray, and nonlinear optical techniques that reveal the different detailed aspects of the interface under in situ conditions in real-time. Furthermore, computational simulations using density functional theory (DFT) and ab initio and classical molecular dynamics (MD) have been critical in uncovering reaction mechanisms at solid–water interfaces, helping to interpret experimental observables and distinguish the reactivities of different surface sites. These studies have shown that surface sites can have stark differences in their reactivities, such as acidity and surface complexation reactions. Importantly, the surface site reactivity also depends on the local environment, i.e., the reactivity of the same surface site differs depending on the structure and identity of its immediate neighbors.

In the last decade, nonlinear optical methods have greatly enhanced our ability to garner molecular information on buried interfaces, i.e., those surfaces under aqueous solutions. Phase-sensitive measurements have yielded complex spectra generated at solid–water interfaces resolving the orientation of the molecules that contribute to the measured response[14,15]. Moreover, theoretical frameworks used to interpret these measurements now separate the contributions from different regions of the interfacial solution layers and assign them to molecules immediately at the buried surface and those at a distance that are still structurally distinct from molecules in the bulk aqueous phase (the diffuse layer)[15,16]. These methods and related approaches have uncovered the details of hydrogen-bonding networks of water immediately adjacent to a surface (in the Stern layer) and how they are perturbed by changes in pH[17] and the addition of aqueous ions[18]. Phase-sensitive measurements have allowed also for the total potential to be quantified directly at the surface[19]. This new capability is important, because the surface potential (ψ) is one of those approximated quantities that must be incorporated into SCMs (Fig. 1). This quantity is often calculated from mean-field models and rarely had been measured experimentally. Now, the surface potential, which differs from the more commonly measured zeta potential, can be ascertained optically, and at arbitrary ionic strength, using heterodyned second harmonic generation (SHG)[19] as well as synchrotron-based X-ray photoelectron spectroscopy (XPS) albeit under more limited conditions[20]. This ability to measure the total surface potential provides an important experimental benchmark for the widely used mean-field models for calculating surface potentials and applying the electrokinetic methods used to quantify interfacial potentials. Ultimately, our ability to assess the electrostatics at the surface without having to invoke classic mean-field models, which often rely on semi-empirical parameters and primitive ion models that were put forth based on less sensitive techniques decades ago, will be critical to develop the next generation of surface models and extend them into SCMs and RTMs.

Advanced techniques for measuring ψ at oxide surfaces still provide an average value for a given interface. However, we know that charged sites on oxide surfaces are localized resulting from protonation and deprotonation of surface hydroxyls. Whether charges are localized or delocalized significantly impacts both the ion distribution and the net water orientation in the interfacial region according to simulations of charged solid–water interfaces[21]. Specifically, charge localization results in ion accumulation at an interface and local re-orientation of water molecules at interfaces compared with the delocalized charged aqueous interface. Furthermore, recent work using Stark spectroscopy indicates that the local fields can vary significantly across the solid–water interface and that interfacial molecules "sample" this heterogeneous, dynamic environment[22].

The interfacial charge structure can be changed drastically by high salinity. Lee et al.[23] observed the salinity-dependent electric double layer (EDL) structure evolution in RbI or RbCl with negatively charged mica surfaces using element-specific resonant anomalous X-ray reflectivity. They found that cations and anions formed alternating discrete layers, causing nonclassical charge overscreening (also referred to as charge reversal) at high salinity. At the silica surface, the impact of overscreening induced by divalent ions with increasing pH on both the water structure and ion speciation within the EDL was also recently observed by Rashwan et al. using vibrational SFG (vSFG) and streaming current measurements[24].

Experimental methods capable of mapping out the local structure with molecular-scale resolution are transformative tools for characterizing the chemistry of solid–water interfaces[7]. Scanning probe measurements over nearly atomically flat surfaces, such as mica[25], paired with finite-element analysis[26] have yielded topographic information on the molecular-scale of both the interfacial potential and water structure. Such methods have been extended to mapping of organic molecules deposited on metal surfaces[27]. Charge profiling three-dimensional (3D) atomic force microscopy has revealed charge layering of ionic liquids on electrodes at Ångstrom depth resolution[28]. 3D fast-force mapping can also estimate the position of individual water molecules in the Stern layer although this emerging method is complicated by data convolution concerns related to tip-specific effects[29]. Other imaging methods such as transmission electron microscopy (TEM), including scanning (STEM), high-resolution (HRTEM), and liquid cell (in situ TEM), in combination with electron energy loss spectroscopy can directly quantify surface structures in dry, humid, or aqueous conditions. Because these measurements are spatially resolved and have near-molecular-scale resolution, they can map out the variety of reactive surface sites on oxide surfaces allowing the abundance of a certain type of surface site to be linked to observable macroscopic reactivities. A well-studied example of this phenomenon is the uptake and release of O_2 by ceria (CeO_2) nanoparticles that are widely used in catalysis and other applications. Combined TEM and modeling studies for CeO_2 have shown that the energetics of O_2 uptake/release is controlled by (1) specific facets (crystallographic orientation), (2) oxygen site vacancies produced during Ce^{3+}/Ce^{4+} redox reaction, and (3) surface hydration (Fig. 3, from ref. [30], and ref. [2]). Because surface defects often produce high energy reactive sites, the emerging research field of defect engineering for nanomaterials is critically tied to these new high-resolution measurements.

Fig. 3: Surface structures of ceria (CeO_2) nanoparticles.

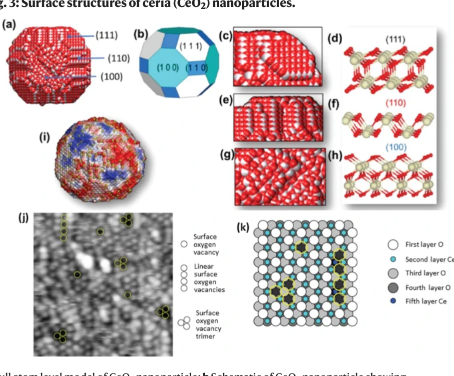

a Full atom level model of CeO_2 nanoparticle; **b** Schematic of CeO_2 nanoparticle showing crystallographic surfaces; **c** Enlarged view of the CeO_2 (111) surface showing the presence of surface steps and corners; **d** Perfect (111) surface of CeO_2 crystal; **e** Nanostructured (110) surface; **f** Perfect (110) surface; **g** Nanostructured (100) surface; **h** perfect (100) surface. Ce = white, O = red; **i** Visualization of catalytic activity of a CeO_2 nanoparticle surface, where oxygen atoms are colored by their lability—the energetic cost of their removal from the surface. Red-white-blue gradient scale, where red corresponds to labile oxygen (energetically easy to extract) and blue corresponds to oxygen ions that are difficult to extract. The yellow spheres are Ce^{3+} species; **j** Scanning tunneling microscopy image of CeO_2 surface, a 6 by 6 nm^2 square is shown from reference[105]; **k** corresponding structural model. Adapted with permission from ref. [2] and ref. [105].

Full size image

Inevitably, the observed heterogeneities of the surface structures discussed above lead to variability in surface properties, such as interfacial potentials, acidities of surface groups (pK_a values)[31,32,33], dissolution rates[10], surface speciation, ion jamming with observed hysteresis in surface acid-base chemistry[33,34], and heterogeneous nucleation patterns across a single surface[35,36] Further complicating the situation is the recognition that the surfaces of some materials, e.g., SiO_2, can have *localized* hydrophilic and hydrophobic regions[36,37,38] that have been proposed to produce different surface acidity constants[39] in concert with changes in hydrogen bonding effects on the distribution of silanol site acidities[40].

Capturing the acidity of surface groups is of specific interest to SCM and RTM development because site charge influences surface reactivity and may vary greatly on the same surface[41,42,43]. A recent significant and surprising finding by ref. [41]. who combined non-contact AFM measurements and DFT modeling indicates that surface hydroxyl groups at an In_2O_3 (111) surface have pK_a values varying several orders of magnitude, based on the H-bond strength measurements at individual surface sites (Fig. 4). Multiple distinct pK_a values have also been observed for silica in both theory and experiment under aqueous conditions[31,39,40]. Therefore, the relative abundance of different sites varies significantly, which we propose should be represented as a probability curve in continuum models.

Fig. 4: Probing individual hydroxyls on In_2O_3 surface with an Atomic Force Microscopy tip.

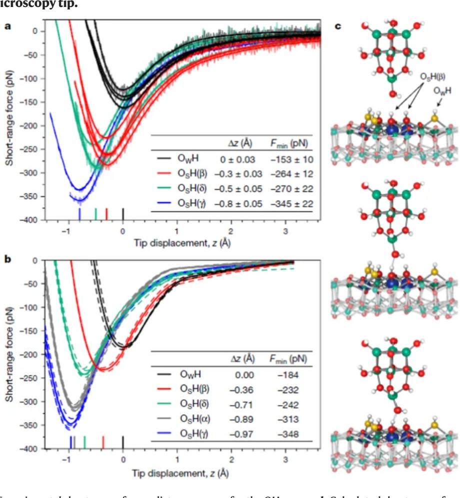

a Experimental short-range force–distance curves for the OH groups; **b** Calculated short-range force–distance curves for the OH groups; **c** Tip–sample configuration for various tip-surface separations. O_W, yellow; H, white; O, red; In, blue and green. Reprinted from reference[41] with permission from Springer Nature, © Wagner et al. under exclusive license to Springer Nature Limited 2021.

Full size image

Although imaging surface structures, localized surface potentials, local pK_a values, and particle–particle interactions are paramount to understanding these systems, it is equally crucial to capture time-dependent fluctuations referred to as surface dynamics. Most environmental interfaces are intrinsically dynamic and sensitive to changes in pH and the presence of ions as they consist of amphoteric sites that become charged and interact, either in a specific or non-specific manner. Generally, models consider that a given solid will exhibit a trend in affinity towards ions based on its composition. Yet, recent experimental work for the planar[44,45] and nanopore silica–water interfaces[46] reveals that such trends in ion affinity can be significantly altered as the pH is changed. One hypothesis that can qualitatively explain a change in relative ion affinity is that the ions can interact with at least two distinct sites on the silica surface, one charged and one neutral, and as the relative ratio of charged to neutral sites increases with pH so does the affinity for ions in solution[45]. Current work aims to investigate whether revising SCMs to include two-site binding of cations can capture such pH-dependent trends in ion affinities. Furthermore, changes in pH, ion concentrations, and solid chemistries might reveal that a probabilistic approach capturing distributions of affinities, rather than two affinity constants, can better predict such behavior.

Real-world solid–water interfaces must also contend with dynamic chemical and geometric complexities: the composition of the aqueous phase at the solid–water interface is multi-component where competitive adsorption plays an important role in Stern and diffuse layer structures[47]. Continuum-scale models must capture the dynamics and coupled behavior between adsorbates, water, and surface site structures. Furthermore, nanoconfinement of surfaces often leads to anomalous chemistry where interfacial reactivity is dictated by the spatial dimension of the reactive solid–water interface[42,48,49]. In particular, in nanopores, the polarization force between ions and the solid surface at an interface determines ion propensity toward nanoconfined spaces[49].

Capturing interfacial reactivity is further complicated by the fact that the speciation of adsorbed ions, and likely of surface sites[50], can vary with ionic strength and surface coverage. For instance, several classic linear and nonlinear optical measurements as well as atomistic simulations have shown that surfaces functionalized with carboxylic acids remain neutral (uncharged) even at highly basic pH values[51,52,53]. The underlying mechanism is one in which Coulomb repulsion within the surface plane is largely reduced when the carboxylate groups pick up a proton from the aqueous solution to form carboxylic acid dimers, similar to those found in glacial acidic acid (an insulating liquid). A similar phenomenon might be occurring for bare oxides such as silica where a bimodal distribution of acidities has been observed for silanol sites above the point-of-zero-charge[31,32,33]. Likewise, Sr^{2+} as well as some lanthanide cations (nominally 3+ in solution) exist as singly-charged species when they are absorbed to certain surfaces[54,55]. In this case, the underlying mechanism likely involves replacing a water molecule from the ion's hydration sphere with a counter-ion, such as chloride or surface deprotonation to create an OH^- group[56,57]. Sr^{2+} then absorbs as the $[SrCl]^+$ ion pair, which is subject to reduced lateral Coulomb repulsion. SCMs should take this effect into account, but currently do not. This is a problem of exponential sensitivity, as the Boltzmann term governing the surface coverage is raised to the power of the charge of the adsorbed ion. If this charge changes from 3 to 2 or from 2 to 1, the exponential sensitivity indicates a much different surface coverage relative to what is expected from bulk thermodynamics. We note

[illegible]

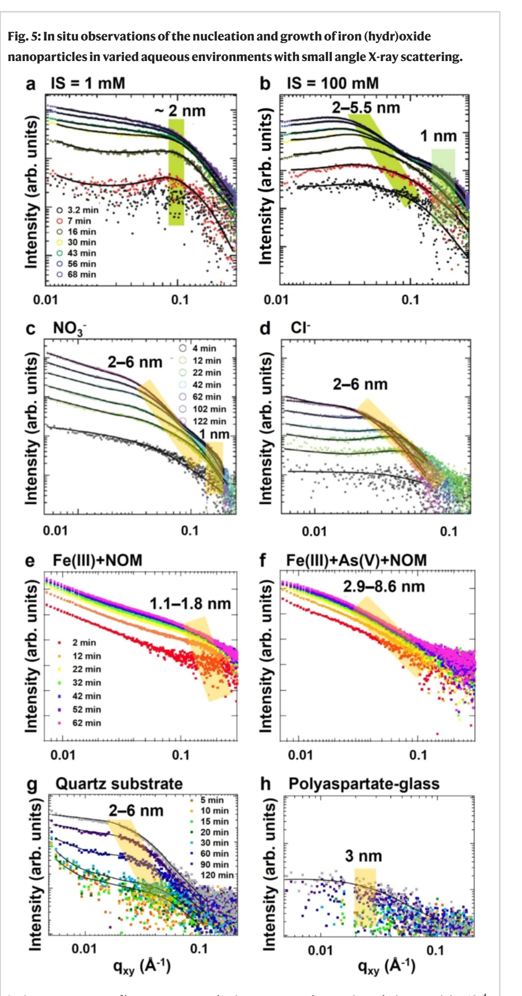

Fig. 6: Heat of adsorption measurements using operando flow microcalorimetry.

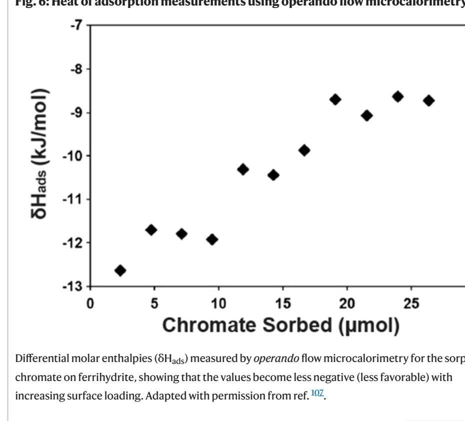

Differential molar enthalpies (δH_{ads}) measured by *operando* flow microcalorimetry for the sorption of chromate on ferrihydrite, showing that the values become less negative (less favorable) with increasing surface loading. Adapted with permission from ref. [80].

Full size image

One promising example is the determination of Fe-oxy(hydr)oxide reactive sites that has been translated into a SCM capable of unifying adsorption equilibrium constants for the important contaminant chromate[82]. Bompoti et al.[82] utilized the MUSE algorithm and found that in SCMs it was easiest to keep the reactive site densities fixed for each solid and vary the solid concentration and capacitance until the model agreed with experimental data. High resolution data, for example using STEM HAADF helps determine the crystal face contributions for different surface sites, and the respective site densities characteristic for each surface that can be incorporated in SCMs[83].

When considering larger scales in RTMs, the dynamic evolution of solid–water interfaces can significantly alter the fate and transport of ions, which is not fully captured in current models. Adsorption of chemical species and temporal evolution of solid phases due to dissolution-precipitation processes changes reactive site densities and types. Until recently, RTM could not include solid nucleation due to the lack of experimental information about nucleation. Instead, it captures precipitation as a group term by assuming that nucleation is instantaneous, and only includes the solid's growth rate. RTMs also do not capture pore-size effects on solubility and nucleation kinetics. Recent advances have been made to incorporate experimentally obtained kinetic and thermodynamic information (e.g., nucleation rates, activation energies, and interfacial energies)[65,84,85] of calcium carbonate nucleation into an RTM code CrunchTope. The incorporation of nanoscale interfacial reactions into the RTM improved the model accuracy of both the evolution of the $Ca(OH)_2$-depleted zone and the surface dissolution zone at supercritical CO_2–brine–cement interfaces (Fig. 7)[69]. Experimentally-obtained nucleation thermodynamic and kinetic information are important in scaling up nanoscale observations of chemical reactions to larger scale predictions. Similarly, this improved RTM framework can be utilized to predict managed aquifer recharge (MAR) where reclaimed water is used to replenish underground reservoirs. The reclaimed water for MAR is rich in dissolved oxygen, which can alter the dissolution of minerals with toxic components such as arsenic-bearing iron sulfides and lead to subsequent iron (hydr)oxide nucleation and toxic species adsorption onto the newly formed iron (hydr)oxides[86,87,88,89]. Understanding the nucleation and dynamic interfacial chemical processes and incorporating them into RTMs will significantly improve the predictions of pollutant mobility, benefiting safer aquifer management to address water shortage problems.

Fig. 7: Incorporation of nanoscale interfacial reactions into a reactive transport model.

a Illustration of direction of CO_2 attack into the cement matrix. The cement samples were reacted in a CO_2-saturated brine (0.5 M NaCl) with a solid-to-liquid volumetric ratio of 1/16. The solution was equilibrated at 95 °C under 100 ± 5 bar of CO_2. A total alteration thickness of 1220 ± 90 μm was observed, including a 960 μm CH ($Ca(OH)_2$, portlandite)-depleted zone, a 100 μm carbonated layer, and a 170 μm surface region. Interfaces between zones are drawn to scale. **b**, **c** Modeling results with and without sufficient consideration of nanoscale mechanisms in comparison with experimental data. **b** Results with no consideration of nanoscale mechanisms. **c** Results with consideration of incomplete filling of pore space at nanoscale, nucleation kinetics, an enhanced solubility in confined pores. By incorporating nanoscale evolution of interfacial chemistry into RTM can generate a better match with experimental observations. Adapted with permission from American Chemical Society from ref. [69].

Full size image

The way forward: towards predicting and controlling interfacial behavior

A logical next step for improving the accuracy of continuum-scale models is to increase the number of discrete parameters used in these models (e.g., use two pK_a values instead of one). Such approaches have already been explored and do indeed show increased accuracy[90]. However, should the splitting of single variables into sets of discrete values (multiple-parameter approach) be the way forward? We argue that it should not be, and a paradigm shift is urgently needed. The fundamental question remains—can we keep applying homogeneous chemistry concepts to heterogeneous systems? The probabilistic nature of chemical phenomena in homogeneous systems has been addressed by statistical mechanics—e.g., the Boltzmann distribution describes the physical nature of molecules in populations having different states, the likelihood of which changes based on the conditions imposed on these populations. Because gaseous or aqueous systems are well-mixed, the Boltzmann distribution is usually Gaussian. When we consider solid surfaces involved in interfacial reactions, a "well-mixed" state is fundamentally impossible for any realistic solid surface. Current molecular models and spatially resolved measurements can capture surface heterogeneity and characterize the localized reactive domains on surfaces at molecular-, nano-, and other scales discussed in "Molecular details matter" section of this Perspective. The problem is that the continuum-scale models, such as SCM and RTMs, are not designed to incorporate spatially differing reactivities of surfaces. We propose that probability distributions of surface descriptors instead of average constant values should be used to formalize interfacial properties in continuum-scale models. Therefore, using probabilities to describe surface properties is a more promising approach in comparison to the stepwise increase in the number of variable values used in multi-parameter sets. Including probability distributions for the variables of interest could result in efficient continuum-scale models because localized effects will be incorporated within non-localized parameterization schemes. Hence, this approach has the potential to address surface heterogeneity at different scales. If successful, this new paradigm will lead to scale-independent, universal models that would allow for the prediction of interfacial reactivities in complex chemical systems for the first time, a dream come true for scientists and engineers in many research fields.

To begin, we need to develop new mathematical frameworks and computational approaches to describe chemical parameters and properties as probability distributions, instead of ensemble average values, to reflect real-world complexity and to generate scaled-up SCMs and RTMs. We propose that accounting for chemical and structural complexity in such new generation SCM and RTM codes requires re-writing them using a fundamentally new approach. As shown in our examples above, reaction rates, equilibrium constants, and surface acidity constants vary across a surface and correlate to distinct structural characteristics (e.g., oxygen vacancies, crystallographic orientation, local structure of amorphous phases, sorbates, and "spectator" ions). We anticipate that normal, bell-shape curves could sufficiently capture the relevant parameter space in some cases where stochastic processes dominate, while in other cases where surface reactivity is a sum of non-random phenomena, they will be best described by more complex types of probability curves. We advocate for applied mathematicians and statisticians to become more involved in interfacial chemistry research to develop rigorous descriptions of interfacial processes for specific use in RTM and SCM codes. The inspiration for such models can be drawn from molecular-scale probabilistic algorithms, including Metropolis Monte Carlo (statistical sampling of energetic states)[91] and Kinetic Monte Carlo (sampling of reaction rates)[92]. These models are currently limited to molecular-scales. From the experimental side, approaches that can quantify the spatiotemporal variation of heterogeneous rates, adsorption free energies, as well as interfacial capacitance, relative permittivity in the Stern layer, and distribution of electric fields are needed to inform these models.

In the geoscience community, Lüttge and co-authors proposed using stochastic models to capture mineral dissolution processes[93,94,95,96]. This conceptual approach was motivated by high-resolution in situ measurements on carbonate and silicate surfaces in aqueous solutions. These measurements clearly indicate site-dependency and time-dependency of the dissolution rates, where the probability distributions evolve in time (Fig. 8). For calcite surfaces in Fig. 8, we see that the initial surface topography has a measurable impact on the mean rate values (peaks in the distribution curves) and on the width of the distributions. In fact, a dissolution rate is more accurately represented by a term "rate spectra," given the variability and gradual changes across a given crystalline surface[10]. Importantly, Lüttge et al. developed an initial framework for treating dissolution phenomena using a probabilistic approach with the dissolution probability defined as[96]:

$$P_{i}=\prod_{j=1}^{i}P_{j} \qquad (1)$$

Fig. 8: Probability distributions of calcite dissolution rates measured in laboratory dissolution experiments.

a Dissolution rate spectra for "striated" surface; and **b** Dissolution rate spectra for "hill-and-valley" surface. Adapted with permission from Trindade Pedrosa et al.[95].

Full size image

Here, P_{i} is the dissolution probability for a molecule with *i* bonds to the surface written as the product of hydrolysis probabilities over all bonds. Furthermore, the logarithm of probability for an individual surface unit to be dissolved is proportional to the sum of activation energies for bond hydrolysis ΔE_{ij}[93]:

$$\ln P_{i}=-\frac{\sum_{j=i}^{i}\Delta E_{ij}}{kT} \qquad (2)$$

where *k* is the Boltzmann constant, and *T* is temperature. We must note that the variability in the measured dissolution rates shown in Fig. 8 is 2 to 3-fold, because these measurements were conducted on the same crystallographic surface. For numerous solids, the difference in dissolution rates for different crystallographic terminations may reach orders of magnitude. Therefore, for realistic solids the probability weighted approach is crucial, because averaging and ignoring this variability may result in model predictions that are "off" by orders of magnitude.

Guren et al.[97] illustrate how to derive a set of dissolution rate probabilities from Kinetic Monte Carlo simulations and then how to use them as input into the macroscopic stochastic model. The result of this rigorous procedure is an accurate representation of mineral dissolution that takes place at different surfaces and surface sites of the same material. Regarding RTM, an approach for parameterizing heterogeneity in surface reactivity has been recently demonstrated using nanotopographic images to generate a distribution of surface slope factors that act as a correction factor for the RTM-calculated rates. This approach led to much better agreement between the simulated dissolution rate maps and rate spectra than the standard RTM[98,99]. While these examples are extremely promising and represent an advance in the field of reaction modeling, the results are still limited to simple systems. A major break-through is needed for translating chemical knowledge from molecular-scale into continuum-scale models.

In this Perspective we propose that an approach that captures probability distributions must be applied in SCMs and RTMs to encompass *all relevant constants and surface properties*, including dissolution rates and nucleation and growth rates, when considering chemistry of solid–water interfaces (Fig. 9).

Fig. 9: Probabilistic nature of surface sites and their reactivities.

Schematic representation of various surface structures on a single crystal surface that have reactivities best represented by a distribution of equilibrium constants (K) and rection rate constants (k). These dynamic surface reactions include solvation, surface complexation, and attachment-detachment processes due to dissolution or precipitation. Chemistry of solid-water interfaces is crucial for understanding environmental fate and transport, and for applications such as water treatment, conventional and unconventional energy, and agriculture (all of which are represented with symbols in the upper portion of the figure).

Full size image

Developing new methods for incorporating probability distributions into SCM and RTM codes for the numerous reactive surfaces present in the environment will be possible by utilizing new computational approaches. A longstanding grand challenge in computational science has been the seamless transfer of information across scales from molecular to field-scales[100]. In practice, this ideal has not been achieved because funding for multi-scale modeling efforts have not been the norm and computational limits have not allowed significant overlap in spatiotemporal scales among the various approaches. The latter obstacle can be overcome with the advent of exascale computing and the development of codes that incorporate machine learning (ML)-based interatomic potentials or ML-IAPs[101]. Connecting atomistic and pore scale simulations through advanced computational power can be achieved by systematic development of interatomic potentials via machine-learning. Exascale computing makes simulations of 10^7 atoms over durations of microseconds possible, and the ML techniques allow for the development of accurate, reactive IAPs based on experimental data and quantum results. Thus, it would be possible to perform atomistic simulations that overlap with the mesoscale and can more realistically represent solid–water interfaces. Exascale computers will allow for accurate atomistic simulations of reactions and flow on scales that overlap the micron-scale elemental volumes of lattice Boltzmann simulations[102]. Coarse-grained mesoscale simulations (i.e., mesoscale) allow for larger and longer spatiotemporal scales that overlap finite element and continuum methods. This "bottom-up" approach can provide parameters that are useful in larger scale models such as SCM (e.g., ref. [103]). Additionally, ML can be used to identify feature importance, value clustering, and detecting anomalous values[104], all of which can aid in the statistical descriptions of interfacial reactivities. Smaller scale simulations can be used to test assumptions and approximations made for larger scale simulations while simultaneously providing chemical mechanism information that could be incorporated into SCMs or RTMs. By incorporating probability distributions and integrating across scales with experiments and simulations, it will become possible to derive new modeling paradigms that are consistent with field observations and incorporate molecular-level information. This approach will enable bridging of laboratory experiments with modeling efforts to predict chemical transformation in complex industrial systems and natural environments, including critical settings such as nuclear waste sites. Similar approaches can be used for predicting catalyst performance and to design fit-for-purpose materials for energy and the environment. With exponentially rising computational power, the advancement in machine learning and artificial intelligence tools and the increasing spatiotemporal resolution of laboratory measurements, this perspective provides a conceptual framework that could enable sustainable solutions to global problems including clean water, renewable energy, and climate change.

References

1. Epsztein, R., DuChanois, R. M., Ritt, C. L., Noy, A. & Elimelech, M. Towards single-species selectivity of membranes with subnanometre pores. *Nat. Nanotechnol.* **15**, 426–436 (2020).

Article CAS PubMed ADS Google Scholar

2. Seal, S. et al. Engineered defects in cerium oxides: tuning chemical reactivity for biomedical, environmental, & energy applications. *Nanoscale* **12**, 6879–6899 (2020).

Article CAS PubMed Google Scholar

3. Jun, Y.-S. Catalyst The roles of chemistry in clean water for all. *Chem* **9**, 1335–1339 (2023).

Article CAS Google Scholar

4. Gonella, G. et al. Water at charged interfaces. *Nat. Rev. Chem.* **5**, 466–485 (2021).

Article CAS PubMed Google Scholar

5. Qin, F. & Beckingham, L. E. The impact of mineral reactive surface area variation on simulated mineral reactions and reaction rates. *Appl. Geochem.* **124**, 104852 (2021).

Article CAS Google Scholar

6. Sun, Y. & Li, Y. Application of surface complexation modeling on adsorption of uranium at water-solid interface: a review. *Environ. Pollut.* **278**, 116861 (2021).

Article CAS PubMed Google Scholar

7. Bañuelos, J. L. et al. Oxide–and silicate–water interfaces and their roles in technology and the environment. *Chem. Rev.* **123**, 6413–6544 (2023).

8. Xu, T., Zheng, L. & Tian, H. Reactive transport modeling for CO_2 geological sequestration. *J. Petroleum Sci. Eng.* **78**, 765–777 (2011).

9. Li, L. et al. Toward catchment hydro-biogeochemical theories. *Wiley Interdiscip. Rev. Water* **8**, e1495 (2021).

Article Google Scholar

10. Fischer, C., Arvidson, R. S. & Lüttge, A. How predictable are dissolution rates of crystalline material? *Geochim. et Cosmochim. Acta* **98**, 177–185 (2012).

11. Reeves, D. & Rothman, D. H. Age dependence of mineral dissolution and precipitation rates. *Glob. Biogeochem. Cycles* **27**, 906–919 (2013).

Article CAS Google Scholar

12. Zhu, C. et al. Testing hypotheses of albite dissolution mechanisms at near-equilibrium using Si isotope tracers. *Geochim. et. Cosmochim. Acta* **303**, 15–37 (2021).

Article CAS ADS Google Scholar

13. Schaefer, J., Backus, E. H. & Bonn, M. Evidence for auto-catalytic mineral dissolution from surface-specific vibrational spectroscopy. *Nat. Commun.* **9**, 3316 (2018).

Article PubMed PubMed Central ADS Google Scholar

14. Myalitsin, A., Urashima, S.-H., Nihonyanagi, S., Yamaguchi, S. & Tahara, T. Water structure at the buried silica/aqueous interface studied by heterodyne-detected vibrational sum-frequency generation. *J. Phys. Chem. C.* **120**, 9357–9363 (2016).

Article CAS Google Scholar

15. Urashima, S.-h, Myalitsin, A., Nihonyanagi, S. & Tahara, T. The topmost water structure at a charged silica/aqueous interface revealed by heterodyne-detected vibrational sum frequency generation spectroscopy. *J. Phys. Chem. Lett.* **9**, 4109–4114 (2018).

Article CAS PubMed Google Scholar

16. Khatib, R. et al. Water orientation and hydrogen-bond structure at the fluorite/water interface. *Sci. Rep.* **6**, 1–10 (2016).

Article Google Scholar

17. Rehl, B. et al. Water dipole populations in the electrical double layer and their contributions to the total interfacial potential at different surface charge densities. *J. Am. Chem. Soc.* **44**, 16338–16349 (2022).

18. Rehl, B. & Gibbs, J. M. Role of ions on the surface-bound water structure at the silica/water interface: identifying the spectral signature of stability. *J. Phys. Chem. Lett.* **12**, 2854–2864 (2021).

Article CAS PubMed Google Scholar

19. Ma, E. et al. A new imaginary term in the second-order nonlinear susceptibility from charged interfaces. *J. Phys. Chem. Lett.* **12**, 5649–5659 (2021).

Article CAS PubMed Google Scholar

20. Brown, M. A. et al. Determination of surface potential and electrical double-layer structure at the aqueous electrolyte-nanoparticle interface. *Phys. Rev. X* **6**, 011007 (2016).

Google Scholar

21. Dewan, S. et al. Structure of water at charged interfaces: a molecular dynamics study. *Langmuir* **30**, 8056–8065 (2014).

Article CAS PubMed Google Scholar

22. Piontek, S. M. et al. Probing heterogeneous charge distributions at the α-Al_2O_3 (0001)/H_2O interface. *J. Am. Chem. Soc.* **142**, 12096–12105 (2020).

Article CAS PubMed Google Scholar

23. Lee, S. S., Koishi, A., Bourg, I. C. & Fenter, P. Ion correlations drive charge overscreening and heterogeneous nucleation at solid–aqueous electrolyte interfaces. *Proc. Natl Acad. Sci.* **118**, e2105154118 (2021).

Article CAS PubMed PubMed Central Google Scholar

24. Rashwan, M. et al. Structure of the Silica/Divalent electrolyte interface: molecular insight into charge inversion with increasing pH. *J. Phys. Chem. C.* **124**, 26973–26981 (2020).

Article MathSciNet CAS Google Scholar

25. Nakouzi, E. et al. Moving beyond the solvent-tip approximation to determine site-specific variations of interfacial water structure through 3D force microscopy. *J. Phys. Chem. C* **125**, 1282–1291 (2021).

26. Yang, T., Meyer, B. W., [illegible] & [illegible]. [illegible]

27. Hapala, P. et al. Mapping the electrostatic force field of single molecules from high-resolution scanning probe images. *Nat. Commun.* **7**, 1–8 (2016).

28. Bonagiri, L. K. S. et al. Real-space charge density profiling of electrode–electrolyte interfaces with angstrom depth resolution. *ACS Nano* **16**, 19594–19604 (2022).

29. Nakouzi, E. et al. Moving beyond the solvent-tip approximation to determine site-specific variations of interfacial water structure through 3D force microscopy. *J. Phys. Chem. C* **125**, 1282–1291 (2021).

30. Sayle, T. X. et al. Structure–activity map of ceria nanoparticles, nanocubes, and mesoporous architectures. *Chem. Mater.* **28**, 7287–7295 (2016).

31. Ong, S., Zhao, X. & Eisenthal, K. B. Polarization of water molecules at a charged interface: second harmonic studies of the silica/water interface. *Chem. Phys. Lett.* **191**, 327–335 (1992).

32. Azam, M. S., Weeraman, C. N. & Gibbs-Davis, J. M. Specific cation effects on the bimodal acid–base behavior of the silica/water interface. *J. Phys. Chem. Lett.* **3**, 1269–1274 (2012).

33. Darlington, A. M. & Gibbs-Davis, J. M. Bimodal or trimodal? The influence of starting pH on site identity and distribution at the low salt aqueous/silica interface. *J. Phys. Chem. C* **119**, 16560–16567 (2015).

34. Gibbs-Davis, J. M., Kruk, J. J., Konek, C. T., Scheidt, K. A. & Geiger, F. M. Jammed acid–base reactions at interfaces. *J. Am. Chem. Soc.* **130**, 15444–15447 (2008).

Article CAS PubMed Google Scholar

35. Jun, Y.-S. et al. Classical and nonclassical nucleation and growth mechanisms for nanoparticle formation. *Annu. Rev. Phys. Chem.* **73**, 453–477 (2022).

Article CAS PubMed ADS Google Scholar

36. Jun, Y. S., Kim, D. & Neil, C. W. Heterogeneous nucleation and growth of nanoparticles at environmental interfaces. *Acc. Chem. Res.* **49**, 1681–1690 (2016).

Article CAS PubMed Google Scholar

37. Isaienko, O. & Borguet, E. Hydrophobicity of hydroxylated amorphous fused silica surfaces. *Langmuir* **29**, 7885–7895 (2013).

Article CAS PubMed Google Scholar

38. Cyran, J. D. et al. Molecular hydrophobicity at a macroscopically hydrophilic surface. *Proc. Natl Acad. Sci.* **116**, 1520–1525 (2019).

Article CAS PubMed PubMed Central ADS Google Scholar

39. Leung, K., Nielsen, I. M. & Criscenti, L. J. Elucidating the bimodal acid–base behavior of the water–silica interface from first principles. *J. Am. Chem. Soc.* **131**, 18358–18365 (2009).

Article CAS PubMed Google Scholar

40. Pfeiffer-Laplaud, M., Costa, D., Tielens, F., Gaigeot, M.-P. & Sulpizi, M. Bimodal acidity at the amorphous silica/water interface. *J. Phys. Chem. C.* **119**, 27354–27362 (2015).

Article CAS Google Scholar

41. Wagner, M., Meyer, B., Setvin, M., Schmid, M. & Diebold, U. Direct assessment of the acidity of individual surface hydroxyls. *Nature* **592**, 722–725 (2021).

Article CAS PubMed ADS Google Scholar

42. Macias-Romero, C., Nahalka, I., Okur, H. I. & Roke, S. Optical imaging of surface chemistry and dynamics in confinement. *Science* **357**, 784–788 (2017).

Article CAS PubMed Google Scholar

43. Kwon, K. D., Vadillo-Rodriguez, V., Logan, B. E. & Kubicki, J. D. Interactions of biopolymers with silica surfaces: force measurements and electronic structure calculation studies. *Geochim. et. Cosmochim. Acta* **70**, 3803–3819 (2006).

Article CAS ADS Google Scholar

44. DeWalt-Kerian, E. L. et al. pH-dependent inversion of Hofmeister trends in the water structure of the electrical double layer. *J. Phys. Chem. Lett.* **8**, 2855–2861 (2017).

Article CAS PubMed Google Scholar

45. Schwierz, N., Horinek, D., Sivan, U. & Netz, R. R. Reversed Hofmeister series—The rule rather than the exception. *Curr. Opin. Colloid Interface Sci.* **23**, 10–18 (2016).

Article CAS Google Scholar

46. Ilgen, A. G., Leung, K., Criscenti, L. J. & Greathouse, J. A. Adsorption at nanoconfined solid–water interfaces. *Annu. Rev. Phys. Chem.* **74**, 169–191 (2023).

47. Sit, I., Wu, H. & Grassian, V. H. Environmental aspects of oxide nanoparticles: probing oxide nanoparticle surface processes under different environmental conditions. *Annu. Rev. Anal. Chem.* **14**, 489–514 (2021).

Article CAS Google Scholar

48. Ilgen, A. G. et al. Defining silica–water interfacial chemistry under nanoconfinement using lanthanides. *Environ. Sci. Nano* **8**, 432–443 (2021).

Article CAS Google Scholar

49. Zhu, Y. et al. Ionic surface propensity controls pH in nanopores. *Chem* **8**, 1–15 (2022).

Article Google Scholar

50. Azam, S., Darlington, A. & Gibbs-Davis, J. M. The influence of concentration on specific ion effects at the silica/water interface. *J. Phys. Condens. Matter* **26**, 244107 (2014).

Article PubMed Google Scholar

51. Konek, C. T. et al. Interfacial acidities, charge densities, potentials, and energies of carboxylic acid-functionalized silica/water interfaces determined by second harmonic generation. *J. Am. Chem. Soc.* **126**, 11754–11755 (2004).

Article CAS PubMed Google Scholar

52. Gershevitz, O. & Sukenik, C. N. In situ FTIR-ATR analysis and titration of carboxylic acid-terminated SAMs. *J. Am. Chem. Soc.* **126**, 482–483 (2004).

Article CAS PubMed Google Scholar

53. Winter, N., Vieceli, J. & Benjamin, I. Hydrogen-bond structure and dynamics at the interface between water and carboxylic acid-functionalized self-assembled monolayers. *J. Phys. Chem. B* **112**, 227–231 (2008).

Article CAS PubMed Google Scholar

54. Jordan, D. S., Saslow, S. A. & Geiger, F. M. Exponential sensitivity and speciation of Al (III), Sc (III), Y (III), La (III), and Gd (III) at fused silica/water interfaces. *J. Phys. Chem. A* **115**, 14438–14445 (2011).

Article CAS PubMed Google Scholar

55. Malin, J. N., Holland, J. G. & Geiger, F. M. Free energy relationships in the electric double layer and alkali earth speciation at the fused silica/water interface. *J. Phys. Chem. C.* **113**, 17795–17802 (2009).

Article CAS Google Scholar

56. Criscenti, L. J. & Sverjensky, D. A. The role of electrolyte anions (ClO 4-, NO 3-, and Cl-) in divalent metal (M 2 +) adsorption on oxide and hydroxide surfaces in salt solutions. *Am. J. Sci.* **299**, 828–899 (1999).

Article CAS ADS Google Scholar

57. Zhang, Z. et al. Structure of hydrated Zn2+ at the rutile TiO2 (110)-aqueous solution interface: Comparison of X-ray standing wave, X-ray absorption spectroscopy, and density functional theory results. *Geochim. et. Cosmochim. Acta* **70**, 4039–4056 (2006).

Article CAS ADS Google Scholar

58. Soderholm, L., Skanthakumar, S. & Wilson, R. E. Structures and energetics of erbium chloride complexes in aqueous solution. *J. Phys. Chem. A* **113**, 6391–6397 (2009).

Article CAS PubMed Google Scholar

59. Dove, P. M. The dissolution kinetics of quartz in sodium chloride solutions at 25 degrees to 300 degrees C. *Am. J. Sci.* **294**, 665 (1994).

Article CAS ADS Google Scholar

60. Icenhower, J. P. & Dove, P. M. The dissolution kinetics of amorphous silica into sodium chloride solutions: effects of temperature and ionic strength. *Geochim. et. Cosmochim. Acta* **64**, 4193–4203 (2000).

Article CAS ADS Google Scholar

61. Kubicki, J. D., Sofo, J. O., Skelton, A. A. & Bandura, A. V. A new hypothesis for the dissolution mechanism of silicates. *J. Phys. Chem. C.* **116**, 17479–17491 (2012).

Article CAS Google Scholar

62. Dewan, S., Yeganeh, M. S. & Borguet, E. Experimental correlation between interfacial water structure and mineral reactivity. *J. Phys. Chem. Lett.* **4**, 1977–1982 (2013).

Article CAS PubMed Google Scholar

63. DelloStritto, M., Piontek, S. M., Klein, M. L. & Borguet, E. Relating interfacial order to sum frequency generation with Ab initio simulations of the aqueous Al2O3 (0001) and (1120) interfaces. *J. Phys. Chem. C.* **122**, 21284–21294 (2018).

Article CAS Google Scholar

64. Tuladhar, A. et al. Ions tune interfacial water structure and modulate hydrophobic interactions at silica surfaces. *J. Am. Chem. Soc.* **142**, 6991–7000 (2020).

Article CAS PubMed Google Scholar

65. Li, Q. & Jun, Y.-S. Salinity-induced reduction of interfacial energies and kinetic factors during calcium carbonate nucleation on quartz. *J. Phys. Chem. C.* **123**, 14319–14326 (2019).

Article CAS Google Scholar

66. Jun, Y. S., Lee, B. & Waychunas, G. A. In situ observations of nanoparticle early development kinetics at mineral-water interfaces. *Environ. Sci. Technol.* **44**, 8182–8189 (2010).

Article CAS PubMed ADS Google Scholar

67. Neil, C. W., Lee, B. & Jun, Y. S. Different Arsenate and Phosphate incorporation effects on the nucleation and growth of Iron(III) (Hydr)oxides on quartz. *Environ. Sci. Technol.* **48**, 11883–11891 (2014).

Article CAS PubMed ADS Google Scholar

68. Ray, J. R., Lee, B., Baltrusaitis, J. & Jun, Y. S. Formation of Iron(III) Hydroxides on Polyaspartate- and Alginate-Coated SiO_2: effects of substrate hydrophilicity and functional groups at the surface. *Environ. Sci. Technol.* **46**, 13167–13175 (2012).

Article CAS PubMed ADS Google Scholar

69. Li, Q., Steefel, C. I. & Jun, Y. S. Incorporating nanoscale effects into a continuum-scale reactive transport model for CO_2-Deteriorated Cement. *Envir. Sci. Tech.* **51**, 10861–10871 (2017).

Article CAS Google Scholar

70. Givens, B. E., Diklich, N. D., Fiegel, J. & Grassian, V. H. Adsorption of bovine serum albumin on silicon dioxide nanoparticles: impact of pH on nanoparticle–protein interactions. *Biointerphases* **12**, 02D404 (2017).

Article PubMed PubMed Central Google Scholar

71. Xu, Z. & Grassian, V. H. Bovine Serum Albumin Adsorption on TiO_2 nanoparticle surfaces: effects of pH and coadsorption of phosphate on protein–surface interactions and protein structure. *J. Phys. Chem. C.* **121**, 21763–21771 (2017).

Article CAS Google Scholar

72. Ustunol, I. B., Coward, E. K., Quirk, E. & Grassian, V. H. Interaction of beta-lactoglobulin and bovine serum albumin with iron oxide (α-Fe2O3) nanoparticles in the presence and absence of pre-adsorbed phosphate. *Environ. Sci. Nano* **8**, 2811–2823 (2021).

Article CAS Google Scholar

73. Kim, D. & Grassian, V. H. Attenuated total reflection-fourier transform infrared and atomic force microscopy-infrared spectroscopic investigation of suwannee river Fulvic acid and its interactions with α-FeOOH. *ACS Earth Space Chem.* **6**, 81–89 (2021).

Article ADS Google Scholar

74. Jayalath, S., Wu, H., Larsen, S. C. & Grassian, V. H. Surface adsorption of Suwannee River humic acid on TiO2 nanoparticles: a study of pH and particle size. *Langmuir* **34**, 3136–3145 (2018).

Article CAS PubMed Google Scholar

75. Wheeler, K. E. et al. Environmental dimensions of the protein corona. *Nat. Nanotechnol.* **16**, 617–629 (2021).

Article CAS PubMed ADS Google Scholar

76. Mauvisseau, Q. et al. The multiple states of environmental DNA and what is known about their persistence in aquatic environments. *Environ. Sci. Technol.* **56**, 5322–5333 (2022).

Article CAS PubMed PubMed Central ADS Google Scholar

77. Yalcin, S. E., Legg, B. A., Yeşilbaş, M., Malvankar, N. S. & Boily, J.-F. Direct observation of anisotropic growth of water films on minerals driven by defects and surface tension. *Sci. Adv.* **6**, eaaz9708 (2020).

Article CAS PubMed PubMed Central ADS Google Scholar

78. Le Traon, C., Aquino, T., Bouchez, C., Maher, K. & Le Borgne, T. Effective kinetics driven by dynamic concentration gradients under coupled transport and reaction. *Geochim. et. Cosmochim. Acta* **306**, 189–209 (2021).

Article ADS Google Scholar

79. Bakaev, V., Bakaeva, T. & Pantano, C. On inverse adsorption chromatography. 2. Determination of isotherms and heats of adsorption as well as energy distributions of adsorption sites. *J. Phys. Chem. C.* **111**, 7473–7486 (2007).

Article CAS Google Scholar

80. Criscenti, L. J. & Sverjensky, D. A. A single-site model for divalent transition and heavy metal adsorption over a range of metal concentrations. *J. Colloid Interface Sci.* **253**, 329–352 (2002).

Article CAS PubMed ADS Google Scholar

81. Kubicki, J. D., Kabengi, N., Chrysochoou, M. & Bompoti, N. Density functional theory modeling of chromate adsorption onto ferrihydrite nanoparticles. *Geochem. Trans.* **19**, 1–12 (2018).

Article Google Scholar

82. Bompoti, N. M., Chrysochoou, M. & Machesky, M. L. A unified surface complexation modeling approach for chromate adsorption on iron oxides. *Environ. Sci. Technol.* **53**, 6352–6361 (2019).

Article CAS PubMed ADS Google Scholar

83. Livi, K. J., Villalobos, M., Ramasse, Q., Brydson, R. & Salazar-Rivera, H. S. Surface site density of synthetic goethites and its relationship to atomic surface roughness and crystal size. *Langmuir* **39**, 556–562 (2022).

Article PubMed Google Scholar

84. Li, Q. & Jun, Y.-S. The apparent activation energy and pre-exponential kinetic factor for heterogeneous calcium carbonate nucleation on quartz. *Commun. Chem.* **1**, 56 (2018).

Article ADS Google Scholar

85. Li, Q., Fernandez-Martinez, A., Lee, B., Waychunas, G. A. & Jun, Y.-S. Interfacial energies for heterogeneous nucleation of calcium carbonate on mica and quartz. *Environ. Sci. Technol.* **48**, 5745–5753 (2014).

Article CAS PubMed ADS Google Scholar

86. Neil, C. W. & Jun, Y. S. Fe^{3+} addition promotes Arsenopyrite Dissolution and Iron(III) (Hydr)oxide formation and phase transformation. *Environ. Sci. Technol. Lett.* **3**, 30–35 (2016).

Article CAS Google Scholar

87. Neil, C. W., Yang, Y. J., Schupp, D. & Jun, Y. S. Water chemistry impacts on Arsenic Mobilization from Arsenopyrite dissolution and secondary mineral precipitation: implications for managed aquifer recharge. *Environ. Sci. Technol.* **48**, 4395–4405 (2014).

Article CAS PubMed ADS Google Scholar

88. Wu, X., Bowers, B., Kim, D., Lee, B. & Jun, Y.-S. Dissolved organic matter affects arsenic mobility and Iron(III) (hydr)oxide formation: implications for managed aquifer recharge. *Environ. Sci. Technol.* **53**, 14357–14367 (2019).

Article CAS PubMed ADS Google Scholar

89. Wu, X. et al. Effects of Phosphate, Silicate, and Bicarbonate on Arsenopyrite dissolution and secondary mineral precipitation. *ACS Earth Space Chem.* **4**, 515–525 (2020).

Article CAS ADS Google Scholar

90. Lutzenkirchen, J. *Surface complexation modelling*. (Elsevier, 2006).

91. Metropolis, N. & Ulam, S. The Monte Carlo method. *J. Am. Stat. Assoc.* **44**, 335–341 (1949).

Article CAS PubMed Google Scholar

92. Jansen, A. P. J. *An introduction to kinetic Monte Carlo simulations of surface reactions*. Vol. 856 (Springer, 2012).

93. Zhang, L. & Lüttge, A. Aluminosilicate dissolution kinetics: a general stochastic model. *J. Phys. Chem. B* **112**, 1736–1742 (2008).

Article CAS PubMed Google Scholar

94. Kurganskaya, I. & Luttge, A. Kinetic Monte Carlo simulations of silicate dissolution: model complexity and parametrization. *J. Phys. Chem. C.* **117**, 24894–24906 (2013).

Article CAS Google Scholar

95. Pedrosa, T., Kurganskaya, I., Fischer, C. & Luttge, A. A statistical approach for analysis of dissolution rates including surface morphology. *Minerals* **9**, 458 (2019).

Article CAS ADS Google Scholar

96. Luttge, A., Arvidson, R. S., Fischer, C. & Kurganskaya, I. Kinetic concepts for quantitative prediction of fluid-solid interactions. *Chem. Geol.* **504**, 216–235 (2019).

Article CAS ADS Google Scholar

97. Guren, M. G., Renard, F. & Noiriel, C. Dissolution rate variability at carbonate surfaces: 4D X-ray micro-tomography and stochastic modeling investigations. *Front. Water* **5**, 1185608 (2023).

Article Google Scholar

98. Karimzadeh, L. & Fischer, C. Implementing heterogeneous crystal surface reactivity in reactive transport simulations: the example of calcite dissolution. *ACS Earth Space Chem.* **5**, 2408–2418 (2021).

Article CAS ADS Google Scholar

99. Schabernack, J. & Fischer, C. Improved kinetics for mineral dissolution reactions in pore-scale reactive transport modeling. *Geochim. et. Cosmochim. Acta* **334**, 99–118 (2022).

Article CAS ADS Google Scholar

100. Cygan, R. T. Molecular modeling in mineralogy and geochemistry. *Mol. Modeling Theory. Appl. Geosci.* **42**, 1–35 (2001).

CAS Google Scholar

101. Venkatraman, A., Wilson, M. & Montes de Oca Zapiain, D. Accelerated Predictions of Charge Density Evolution in MD simulations Using Machine Learning. *Bull. Am. Phys. Soc.* Abstract: T18.00013 (2023).

102. Akai, T., Blunt, M. J. & Bijeljic, B. Pore-scale numerical simulation of low salinity water flooding using the lattice Boltzmann method. *J. Colloid Interface Sci.* **566**, 444–453 (2020).

Article CAS PubMed ADS Google Scholar

103. Fitts, J. P. et al. Second-harmonic generation and theoretical studies of protonation at the water/α-TiO2 (1 1 0) interface. *Chem. Phys. Lett.* **411**, 399–403 (2005).

Article CAS ADS Google Scholar

104. Zhong, S. et al. Machine learning: new ideas and tools in environmental science and engineering. *Environ. Sci. Technol.* **55**, 12741–12754 (2021).

CAS PubMed Google Scholar

105. Grinter, D. C., Ithnin, R., Pang, C. L. & Thornton, G. Defect structure of ultrathin ceria films on Pt (111): atomic views from scanning tunnelling microscopy. *J. Phys. Chem. C.* **114**, 17036–17041 (2010).

Article CAS Google Scholar

106. Hu, Y., Lee, B., Bell, C. & Jun, Y. S. Environmentally abundant anions influence the nucleation, growth, ostwald ripening, and aggregation of hydrous Fe(III) oxides. *Langmuir* **28**, 7737–7746 (2012).

Article CAS PubMed Google Scholar

107. Kabengi, N. J., Chrysochoou, M., Bompoti, N. & Kubicki, J. D. An integrated flow microcalorimetry, infrared spectroscopy and density functional theory approach to the study of chromate complexation on hematite and ferrihdyrite. *Chem. Geol.* **464**, 23–33 (2017).

Article CAS ADS Google Scholar

Download references

Acknowledgements

We thank M. Rubio and D. Thompson at Sandia National Laboratories for help with graphics design and editing. We are grateful to the three reviewers, who provided valuable feedback for the proposed concept. A.G.I. was supported by the U.S. Department of Energy, Office of Science, Office of Basic Energy Sciences, Chemical Sciences, Geosciences, and Biosciences Division under Field Work Proposal Number 23-015452. E.B. gratefully acknowledges the support of the National Science Foundation (CHE 2102557). F.M.G. was supported by the US National Science Foundation (CHE- 2153191) and the Department of Energy (DE-SC0023342). V.H.G. research was sponsored by the Army Research Office and was accomplished under Grant Number W911NF-23-1-0181. The views and conclusions contained in this document are those of the authors and should not be interpreted as representing the official policies, either expressed or implied, of the Army Research Office or the U.S. Government. The U.S. Government is authorized to reproduce and distribute reprints for Government purposes notwithstanding any copyright notation herein. Y.S.J. is grateful for the support received from the American Chemical Society's Petroleum Research Fund (62756-ND5) and the U.S. Department of Energy Office of Science (DE-SC0023390). This article has been authored by an employee of National Technology & Engineering Solutions of Sandia, LLC under Contract No. DE-NA0003525 with the U.S. Department of Energy (DOE). The employee owns all right, title and interest in and to the article and is solely responsible for its contents. The United States Government retains and the publisher, by accepting the article for publication, acknowledges that the United States Government retains a non-exclusive, paid-up, irrevocable, world-wide license to publish or reproduce the published form of this article or allow others to do so, for United States Government purposes. The DOE will provide public access to these results of federally sponsored research in accordance with the DOE Public Access Plan https://www.energy.gov/downloads/doe-public-access-plan. This paper describes objective technical results and analysis. Any subjective views or opinions that might be expressed in the paper do not necessarily represent the views of the U.S. Department of Energy or the United States Government.

Author information

Authors and Affiliations

Geochemistry Department, Sandia National Laboratories, Albuquerque, NM, 87123, USA
Anastasia G. Ilgen

Department of Chemistry, Temple University, Philadelphia, PA, 19122, USA
Eric Borguet

Department of Chemistry, Northwestern University, Evanston, IL, 60208, USA
Franz M. Geiger

Department of Chemistry, University of Alberta, Edmonton, AB, T6G 2G2, Canada
Julianne M. Gibbs

Department of Chemistry and Biochemistry, University of California, La Jolla, CA, 92093, USA
Vicki H. Grassian

Department of Energy, Environmental and Chemical Engineering, Washington University in St. Louis, St. Louis, MO, 63130, USA
Young-Shin Jun

Department of Geosciences, Georgia State University, Atlanta, GA, 30302, USA
Nadine Kabengi

Department of Earth, Environmental and Resource Sciences, The University of Texas at El Paso, El Paso, TX, 79968, USA
James D. Kubicki

Contributions

The manuscript was written through contributions of all authors. All authors actively edited all draft versions and the final version of the manuscript. A.G.I. proposed the main concept and led the development of the main argument throughout the manuscript; E.B. wrote the sections relevant to SiO_2 surface chemistry and specific ion effects; F.M.G. and J.M.G. performed calculations on the ionic strength impacts on the Gouy-Chapman Stern potential and wrote the sections on vSFG and SHG spectroscopies; V.H.G. wrote the sections on complex interfaces with organic species and actively participated in the development of the manuscript structure; Y.S.J. wrote the discussion on the nucleation of environmental nanoparticles and the incorporation of nanoscale interfacial reactions into reactive transport modeling; N.K. wrote the section on the variability of adsorption enthalpies with surface coverages; J.D.K. wrote the sections relevant to molecular simulations, and on the new opportunities enabled by exascale computing.

Corresponding author

Correspondence to Anastasia G. Ilgen.

Ethics declarations

Competing interests

The authors declare no competing interests.

Peer review

Peer review information

Nature Communications thanks the anonymous, reviewer(s) for their contribution to the peer review of this work.

Additional information

Publisher's note Springer Nature remains neutral with regard to jurisdictional claims in published maps and institutional affiliations.

Rights and permissions

About this article

Cite this article

Ilgen, A.G., Borguet, E., Geiger, F.M. *et al.* Bridging molecular-scale interfacial science with continuum-scale models. *Nat Commun* **15**, 5326 (2024). https://doi.org/10.1038/s41467-024-49598-y

Download citation

Received	Accepted	Published
27 December 2023	07 June 2024	22 June 2024

DOI
https://doi.org/10.1038/s41467-024-49598-y

Subjects

Computational chemistry Environmental chemistry Geochemistry